www.czasopisma.pan.pl PAN www.journals.pan.pl
Opto-Electronics Review 25 (2017) 55–64

Contents lists available at ScienceDirect

Opto-Electronics Review

journal homepage: http://www.journals.elsevier.com/opto-electronics review

Review

# Top PV market solar cells 2016

E. Płaczek-Popko

*Division of Quantum Technologies, Faculty of Fundamental Problems of Technology, Wroclaw University of Science and Technology, Wybrzeże Wyspiańskiego 27, 50-370 Wroclaw, Poland*

ARTICLE INFO

*Article history:*
Received 16 January 2017
Accepted 6 March 2017
Available online 9 May 2017

*Keywords:*
Photovoltaics
Solar cells
Energy band diagram
Heterojunction

ABSTRACT

Photovoltaic (PV) technologies which play a role in PV market are divided into basic two types: wafer-based (1st generation PV) and thin-film cell (2nd generation PV). To the first category belong mainly crystalline silicon (c-Si) cells (both mono- and multi-crystalline). In 2015 around 90% of the solar market belonged to crystalline silicon. To the 2nd generation solar cells belongs thin film amorphous silicon (a-Si) or a combination of amorphous and microcrystalline silicon (a-Si/μc-Si), compound semiconductor cadmium telluride (CdTe), compound semiconductor made of copper, indium, gallium and selenium (CIS or CIGS) and III–V materials. The PV market for thin film technology is dominated by CdTe and CIGS solar cells. Thin film solar cells' share for all thin film technologies was only 10% in 2015. New emerging technologies, called 3rd generation solar cells, remain the subject of extensive R&D studies but have not been used in the PV market, so far.

In this review the best laboratory 1st and 2nd generation solar cells that were recently achieved are described. The scheme of the layer structure and energy band diagrams will be analyzed in order to explain the boost of their efficiency with reference to the earlier standard designs.



**Contents**

1. Introduction ..... 55
1.1. Shockley - Quiesser limit ..... 56
2. Modern crystalline solar cell ..... 56
3. Thin films solar cells ..... 58
3.1. Homojunction thin films SC ..... 58
3.1.1. III-V junction SC ..... 58
3.1.2. a:Si SC ..... 58
3.2. Heterojunction thin films SC ..... 58
3.2.1. CIGS SC ..... 59
3.2.2. Kesterites ..... 59
3.2.3. CdTe SC ..... 61
3.2.4. Multi-junction SC ..... 61
3.2.5. III–V/Si SC ..... 62
4. New emerging technologies ..... 62
5. Conclusions ..... 62
Acknowledgements ..... 63
References ..... 63

## 1. Introduction

According to the Photovoltaic (PV) Market Alliance (recent report of 15th June, 2016) global PV markets should reach at least 60 GW in 2016 and more than 70 GW in 2017. Thus, by the end of 2016, total installations will reach 321 GW [1]. This forecast has been confirmed by the European Photovoltaic Industry Asso-

*E-mail address:* Ewa.Popko@pwr.edu.pl

http://dx.doi.org/10.1016/j.opelre.2017.03.002
1896-3757/

ciation (EPIA) reports that the 540 GW mark at a global level could be reached by the end of 2019 [2]. The increase in installations is accompanied by falling prices of solar cells. PV Magazine reports that in June 2016 the price of the most efficient modules dropped down to 0.7€/$W_p$, while the mainstream modules (typically with 60 cells, standard aluminum frame, white backsheet and 245–270 $W_p$) cost only about 0.5€/$W_p$ [3]. Here $W_p$ stands for the module power at maximum power point for Standard Test Conditions. These numbers indicate that the PV market is growing rapidly and the prospects for the PV future are extremely promising.

PV technologies are divided into basic two types: wafer-based PV (called 1st generation PV) and thin-film cell PV (called 2nd generation PV). To the first category belong crystalline silicon (c-Si) cells (both single crystalline silicon and multi-crystalline silicon) and gallium arsenide (GaAs) cells. So far silicon solar cells have dominated PV market because of their mature technology. In 2015 around 93% of the solar market belonged to crystalline silicon with 24% – to monocrystalline and 69% to multicrystalline silicon solar cells [4]. Crystalline silicon's share has been rapidly growing during last few years due to the development of Chinese manufacturers.

Since solar cells were invented the scientists have been looking for absorber materials alternative to silicon. The current standard thickness of a crystalline silicon wafer is about 180 μm, but the aim is to reach lower thickness of 100 μm since the pure Si wafer creates the main cost of Si solar cells. Silicon in its pure form (of 99.9999% purity for solar applications) is very expensive and makes up about 20%–25% of the cost of crystalline panels. The thin film technology (2nd generation solar cells) provides alternative absorber materials, such as amorphous silicon (a-Si) or a combination of amorphous and microcrystalline silicon (a-Si/μc-Si), the compound semiconductor cadmium telluride (CdTe), a compound semiconductor made of copper, indium, gallium and selenium (CIS or CIGS) and III–V materials (GaAs, InP and AlGaAs). Solar cells made from these materials are called thin-film solar cells because the absorbers have the thickness of a few micrometers. The semiconductor cost of a thin film silicon is about 2% in thin film panels. The thin film solar cells take advantage in lower costs, but they generally exhibit lower efficiency than crystalline solar cells.

In Europe the PV market for thin film technology is dominated by CdTe and CIGS solar cells. The leader by far in thin film technology is First Solar whose cadmium telluride module manufacturing costs are less than those of most crystalline cell manufacturers.

In the laboratory, high concentration multi-junction solar cells achieve an efficiency of up to 46.0% today [5]. However, due to the high cost of their production, the only entry market is space applications.

Thin film solar cells' share for all thin film technologies was only of 10% in 2015 and it is predicted to drop down to 7% by 2017 according to International Technology Road Map for Photovoltaic (ITRPV) [6]. New emerging technologies, such as organic, dye sensitized, quantum dot and perovskite solar cells (called 3rd generation solar cells) remain the subject of extensive R&D studies but have not been used in PV market, so far.

In the article we shall focus on the best laboratory inorganic 1st and 2nd generation solar cells which are potential candidates for PV market. These are the recently announced top solar cells and those reported by Green et al. in the solar cell efficiency tables (version 48) [5]. The main criterion dictating whether these results were included in the Tables is that they must have been independently measured by a test center listed elsewhere [7]. This review presents current technologies for top high-efficiency 1st and 2nd generation solar cells. In particular the layer structure and energy band diagrams of the solar cells are analyzed in order to shed light on the progress of these technologies and origin of their efficiency improvement.

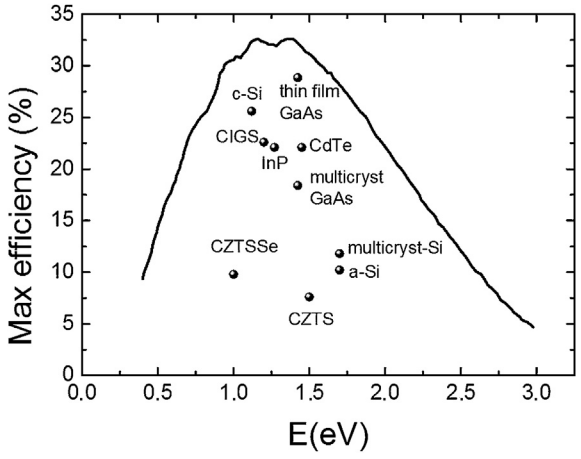


**Fig. 1.** S–Q efficiency curve for a single junction solar cell under AM1.5 illumination from Wiki page. The points represent the best experimental single junction cells fabricated to date.

### 1.1. *Shockley - Quiesser limit*

The efficiency of a solar cell is the main parameter characterizing its operation. The theoretical limit of efficiency for single-junction solar cells is usually referred to as the Shockley–Queisser (SQ) limit [8]. In Fig. 1, the maximum efficiency of a single-junction solar cell calculated using the Shockley–Queisser model as a function of band gap energy is shown. The calculations were made with the assumption that the incident solar spectrum is approximated as a 1.5AMO spectrum, and that one electron–hole pair is excited per incoming photon [9]. The points represent the best experimental single junction cells fabricated to date. In the article the reference to these solar cells is included.

## 2. Modern crystalline solar cell

Silicon solar cells have the advantage of using an absorber material that is stable, non-toxic, abundant and well recognized. It has an energy band gap of 1.12 eV, not far from the optimal value for a solar cell of 1.34 eV [9]. The record 25.0% power conversion efficiency for crystalline silicon solar cells was set by the University of New South Wales (UNSW), Australia, in 1999 [10,11]. This record was broken in 2014, when Panasonic, Japan [12] and SunPower, USA [13], announced independently certified efficiencies of 25.6% and 25.0%, respectively. The theoretical S–Q efficiency limit of a silicon solar cell is 33.5% with the assumption that the radiative recombination dominates [14]. However, silicon is an indirect band gap semiconductor so Auger recombination is dominant instead of the radiative recombination and this results in a lower theoretical limit. As it was shown by Richter et al. a maximum theoretical efficiency equals 29.43% for a 110 μm thick cell made of undoped Si [15]. As it is shown below, the matured technology of silicon solar cells provides the solar cells of efficiency larger than 25%, so it is close to the theoretical limit. Moreover, the efficiency of best modules is close – 24% [5].

The scheme of a conventional crystalline solar cell produced until 1999 is shown in Fig. 2. The cell is made of a p-type silicon wafer, also called an absorber, of thickness of 180–300 μm. N-type layer, called emitter, has much lower thickness (~1 μm). This asymmetry arises from the fact that the carriers generated by the light must reach the junction area before they recombine. Therefore, the thickness of the emitter has to be on the order of diffusion length. The front metal contacts for the cell shown in Fig. 2 form a grid pattern. These contacts collect electrons. The holes are collected at the back contact. Since 1970 the technology of metal contacts is

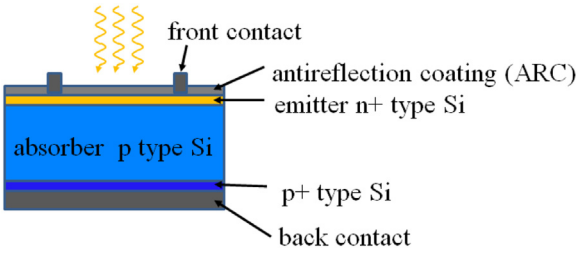


**Fig. 2.** The scheme of a conventional crystalline solar cell.

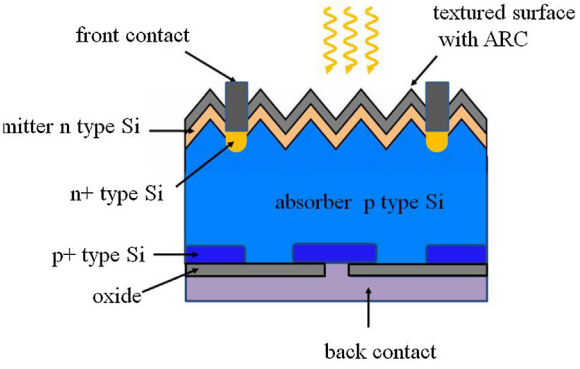


**Fig. 3.** The structure of PERL solar cell.

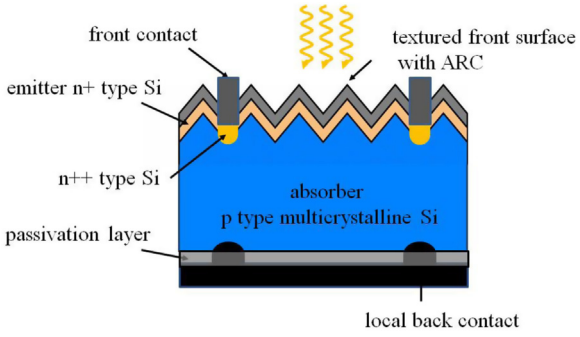


**Fig. 4.** The structure of PERD solar cell (Trina Solar).

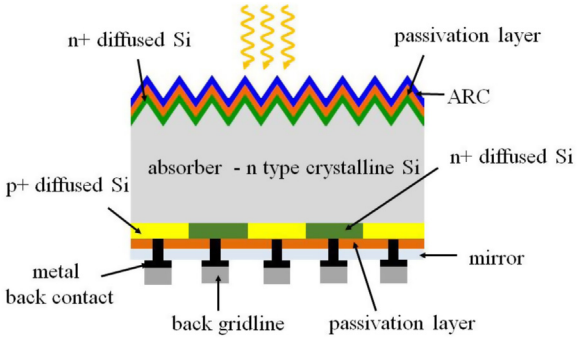


**Fig. 5.** The scheme of an IBC solar cell.

dominated by the screen-printing technique for its simplicity. The top of the solar cell is covered with an antireflection coating (ARC).

Modification of this solution which in 1999 led to the 25% efficiency consisted of the Passivated Emitter Rear Locally (PERL) idea [10]. The PERL concept is based on the minimized optical and collection losses. The top surface is textured with inverted pyramid structures, covered with an antireflection coating (ARC) and photolithography is used to create a metal grid. Light reflected from the pyramid may again fall on the absorber, so that its path length enhances. ARC minimizes light reflection and the metal grid processed by the photolithography reduces the absorber's shading. A bare surface of a c-Si layer contains many dangling bonds which act as recombination centers. In order to reduce the surface recombination, a passivation layer of silicon oxides or silicon nitrides is deposited on top of the emitter and at the rear of the absorber layer. The metal electrodes buried in the passivation layer collect electrons from the emitter. The metal-semiconductor interface is usually defected, therefore it is the source of undesired recombination. In order to avoid this recombination, the area of the interface is minimized. Additionally, the emitter below the interface is heavily doped for a better metal-semiconductor contact.

For the same purpose also in the case of the back contact, the area of the contact is minimized and the highly doped p+ region is realized. The potential barrier at the p+/p interface hinders minority electrons in the p-region from diffusing to the back surface. This effect is called the back surface field (BSF). In the case of the PERL design the p+ doping layer is realized locally (cf. Fig. 3) while in the PERD solar cells, the p+ layer is missing (cf. Fig. 4).

PERD-type technology has become the focus for the mass production for its lower cost, compared with the PERL-type solar cell. In Fig. 4 the structure of the PERD solar cell realized on a p-multicrystalline Si wafer by Trina Solar [16] is shown.

Let us remind that the multicrystalline (polycrystalline) silicon is a material consisted of multiple small silicon crystals. Polycrystalline cells can be recognized by a visible grain, a "metal flake effect". The lower cost of the polycrystalline solar cells compared to the single crystal silicon is related primarily to the cheaper technology of the wafer growth.

Using the interdigitated back contact (IBC) technology, the U.S. company SunPower has demonstrated the efficiency of 25.25 under 1 Sun operation [17]. In the IBC cells the metal grid shading at the front surface is missing (Fig. 5). Both electron and hole collection occurs at the rear side of the device. The back surface consists of interdigitated regions doped with boron or phosphorus. The former selectively collects holes whereas the latter – selectively collects electrons. Hence, the cell structure consists of alternating stripes of n-type and p-type doped regions. It has to be pointed out that in this solution, the wafer may be n-type, as it is shown in the case of the cell presented in Fig. 5. N-type Si material has been proven to be more suitable for IBC solar cells due to its larger tolerance to most common impurities compared to a p-type Si [18]. Moreover, n-type Czochralski (CZ) Si is free of light-induced degradation related to boron–oxygen complexes. Additionally, the passivation layer at the back side is made from the material of low refraction index and acts as a mirror for the longer wavelengths.

Recently [18,19] Trina Solar achieved the record-breaking for an n-type mono-crystalline silicon solar cell fabricated with a process that integrates the advanced Interdigitated Back Contact structure with industrial low-cost processes. The best $156 \times 156\ mm^2$ solar cell fabricated entirely with a screen-printed process reached a total-area efficiency of 23.5%.

Recently a new design of the silicon solar cell has been elaborated. This is the heterojunction with an intrinsic thin layer, called the HIT solar cell. Fig. 6 shows the structure of a two-side contacted HIT solar cell.

The HIT solar cell, is comprised of an intrinsic (i-type) a-Si:H layer and a p-type a-Si:H layer deposited on a randomly textured n-type Czochralski (CZ) crystalline silicon wafer to form a p/n heterojunction and i-type and n-type a-Si:H layers deposited on the opposite side of the wafer. The energy gap of an amorphous hydrogenated Si is in the order of 1.6–1.8 eV depending on the amount of hydrogen. It is a direct band gap semiconductor, thus its optical properties are better compared to crystalline silicon. Hydrogena-

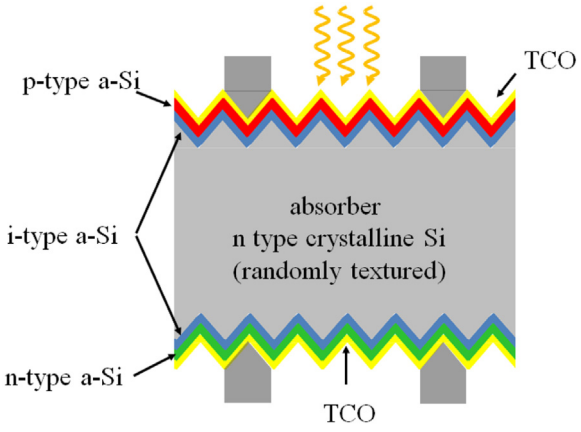


**Fig. 6.** The layer structure of a HIT solar cell.

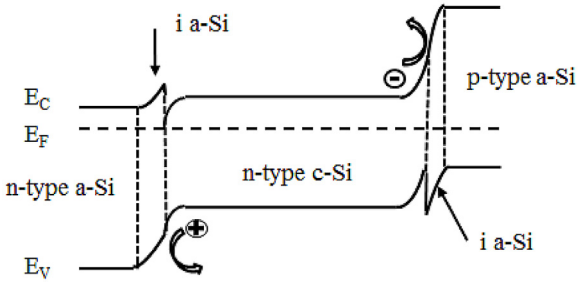


**Fig. 7.** Energy band diagram of a silicon HIT solar cell.

tion is necessary because it leads to passivation of numerous defects in amorphous silicon (around $10^{19}$ cm$^{-3}$) [20].

The thickness of a wafer in the HIT cell is of 150 μm. On both sides of the doped a-Si:H layers, transparent conductive oxide (TCO) layers and metal grid electrodes are fabricated. By inserting the high-quality intrinsic a-Si:H layer between the c-Si wafer and the doped a-Si:H layer using a low-damage process, the surface dangling bonds of c-Si can be well passivated. The advantage of using the wider band gap material is that minority-carrier concentrations are greatly suppressed by the wider bandgap, correspondingly reducing recombination rates.

In Fig. 7 the energy band diagram for of the HIT solar cell with an n-Si wafer is shown. Due to the band gap of a-Si:H and c-Si differing by about 0.5–0.7 eV, offsets between the conduction- and valence bands of a-Si:H and c-Si are present. The state of knowledge is that the valence band offset is larger than the conduction band offset by a factor of 2–3 [21]. The minority carriers – holes are collected in the front side electrode while the majority carriers – electrons are collected in the back side electrode. The thickness of the (i)a-Si:H layer is low enough to prevent holes from trapping at the potential well, so that holes tunnel to the (p)a-Si:H emitter. On the back side, the large valence band offset repels holes from the back contact hindering recombination. The same holds for electrons at the front contact (the arrows in Fig. 7). The small conduction band offset allows efficient for electron collection at the back side contact.

In 2014 Panasonic demonstrated a new world record efficiency of 25.6% by combining their HIT technology with the IBC concept [12].

The review on the modern high efficiency technology of silicon solar cells can be found in the paper by Xiao and Xu [22].

## 3. Thin films solar cells

### 3.1. Homojunction thin films SC

#### 3.1.1. III-V junction SC

In 2012 Alta Devices reached record efficiency (28.85%) of a direct thin film band gap GaAs solar cell. The band gap of GaAs is 1.424 eV, very close to the optimal value for a band gap of a semiconductor material S–Q limit [9]). The theoretical S–Q limit for a GaAs homojunction solar cell equals 33.5% [23]. The record breaking efficiencies were achieved through the phenomenon called photon recycling. In this process photons bounce off the back of the solar cell which allows them to be recaptured by the material and converted to electricity. The structure of the GaAs solar cell is a standard structure as that shown in Fig. 1, with Si material replaced by a GaAs epitaxial layer. Single-crystalline III–V materials are well-suited to exploiting photon recycling, because they can approach near-ideal internal fluorescence yield (i.e. the fraction of absorbed photons that are re-radiated as photons, under open-circuit conditions) [24]. Moreover, in order to optimize the reflection of photons and enhance the photon recycling the thin epitaxial layer of GaAs is separated from the substrate by the lift-off process (ELO process) allowing access to the back of the device.

#### 3.1.2. a:Si SC

Record efficiency of the amorphous silicon solar cell belongs to the Japanese Institute of Advanced Industrial Science and Technology (AIST) and it was announced in 2014 [25]. Typically a:Si solar cells are realized as a p-i-n junction with very thin p and n sides and a thick intrinsic region. The one of record efficiency was also made in the same configuration. The efficiency increase was the result of a modified growth method of absorber [25]. Thin film silicon is usually deposited with a chemical vapour deposition (CVD). This technique was replaced by a remote plasma process using a triode PECVD technique. Due to this modification the suppression of the light-induced degradation of an a-Si:H solar cell was obtained.

In Fig. 8a the layer structure of a:Si:H p-i-n solar cell is shown and in Fig. 8b the energy band diagram.

Transparent conductive oxide is at the front of the cell while at the back of the cell – reflecting contact. The i-region of a p-i-n junction built-in electric field makes electrons and holes move to relevant electrodes. The electrical transport is no longer due to diffusion like in a p-n junction but rather due to drift. This is very important since diffusion length in a hydrogenated amorphous silicon is in the order of 100–300 nm. This short diffusion length is connected with a very high density of defects in an amorphous hydrogenated Si in the order of $10^{16}$ cm$^{-3}$ [26]. The interfaces within the device are rough in order to increase light scattering and effective light path.

Thin solid films silicon solar cells are also made of a hydrogenated nanocrystalline silicon (nc-Si:H) known also as a microcrystalline Si. Record efficiency 11.8% of a microcrystalline Si cell belongs to AIST Company and it was announced in October 2014.

### 3.2. Heterojunction thin films SC

Heterojunction solar cell comprises a window material with a wider band gap and a lower band gap absorber (Fig. 9). The main advantage of the heterojunction solar cell is that the front surface recombination does not affect its operation because the window is transparent for the photons of energy less than the band gap of the absorber. The disadvantage is the heterojunction itself because of an interface recombination and band edge discontinuities at interface.

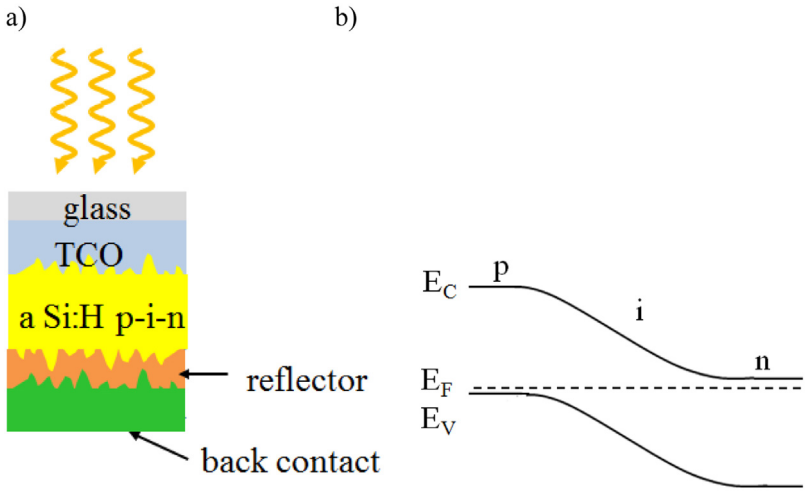


**Fig. 8.** (a) The scheme of a:Si:H p-i-n solar cell and (b) corresponding energy band diagram.

*3.2.1. CIGS SC*

Germany's Center for Solar Energy and Hydrogen Research Baden-Württemberg (ZSW) announced in June 2016 that it had set a new world record for thin film solar technology with a 22.6% efficient solar PV cell based on a semiconducting chalcopyrite $Cu(In_xGa_{1-x})Se_2$, copper indium gallium diselenide (CIGS) technology [27]. The efficiency was verified by the Fraunhofer Institute for Solar Energy Systems (ISE). ZSW achieved the 22.6% efficiency on a 0.5 square centimeter test cell. The boost of efficiency was achieved i.e. by the post-deposition treatment of the CIGS surface with alkaline metal compounds being incorporated into this layer. ZSW has beaten the record achieved by an Hanergy's Solibro cell of efficiency equal to 21%, announced in June 2014 [28].

Standard layer structure and energy band diagram for the CIGS solar cell is shown in Fig. 10. The absorber layer comprises of p-type polycrystalline CIGS (typically 2 μm thick) grown on glass (preferably lima-glass) substrate covered with a molybdenum layer. The latter accomplishes back ohmic contact. On top of the absorber a CdS buffer layer of 50 nm thickness is deposited. It serves as the n partner for the p-CIGS side of a heterojunction. The CdS layer is followed by ZnO and subsequently ZnO:Al layers. The ZnO:Al is a transparent conductive oxide (TCO) providing front contact. Typically $Cu(In_xGa_{1-x})Se_2$ with $x = 0.2–0.3$ of energy gap equal to 1.1–1.2 eV is used [29] and it forms a heterojunction with CdS of energy gap equal to 2.5 eV. In Fig. 10b the band diagram of the CIGS heterojunction is shown. The crucial parameters – valence band and conduction band offsets between CIGS and CdS were found to be equal to 0.9 eV and, therefore, a conduction band offset of 0.45 eV [30]. The conduction band offset between the buffer and the ZnO window was determined to be 0.4 eV [31]. The role played by each of the layers is explained in Ref. [32] and recent review on the energy band alignment in chalcogenide thin film solar cells is given in Ref. [33].

The success of high efficiency of CIGS solar cells started when it was found that sodium coming from the glass substrate diffusing into an absorber is responsible for efficiency boost [34]. The role that alkali ions play in CIGS solar cells is still under debates, however it is known that it leads to a reduced recombination rate in the absorber and enhanced the open circuit voltage $V_{oc}$. The absorber is a polycrystalline material and, therefore, the grain boundaries are the source of undesired recombination centres. In Ref. [35] the CIGS solar cells with post-deposition treatment (PDT) using NaF and KF were studied and it was shown that whereas Na is more effective in increasing the hole concentration in CIGS, K significantly improves the pn-junction quality. The beneficial role of K in improving the PV performance is attributed to a reduced recombination at the CdS/CIGS interface [35].

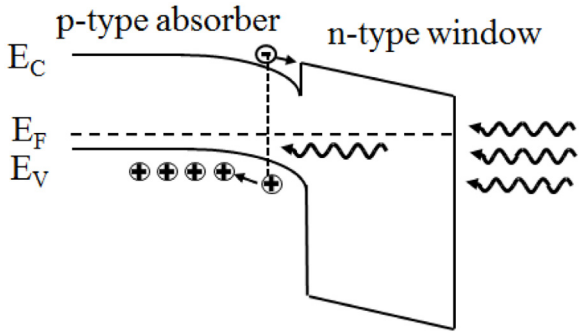


**Fig. 9.** Energy band diagram of a HJ thin film solar cells.

CIGS solar cells may be deposited on flexible substrates. In this case Na is incorporated by the use of Na-containing precursors. Very recently, efficiencies above 20% have been achieved with flexible polyimide substrates using a potassium fluoride post-deposition treatment (KF PDT) [36].

*3.2.2. Kesterites*

Indium, a crucial component in CIGS solar cells is a very rare element. Therefore, many researchers focused on finding new materials that could replace indium. Kesterite $Cu_2ZnSn(S_{1-x}Se_x)_4$ (CZTSSe) compounds are very promising because the raw material costs are extremely low, the elements are abundant and non-toxic. Their band gap may be tuned from 1.0 eV ($Cu_2ZnSnSe_4$) to 1.5 eV ($Cu_2ZnSnS_4$) and absorption coefficient is higher than $10^4$ cm$^{-1}$. In April 2016 IMRA Europe announced a new record efficiency 9.8% of a CZTSSe solar cell [37] and University of New South Wales, Australia [36] – 7.6% of a CZTS solar cell. In the former case, the solar cells with Al/ITO/ZnO/CdS/CZTSSe/Mo-glass structure were fabricated employing a fast and low-cost technology using an aqueous ink deposited by a nonpyrolytic spray, followed by high temperature crystallization and selenization steps [37]. In the latter case the boost in efficiency was obtained by utilizing $Zn_{1-x}Cd_xS$ film instead of a traditional CdS buffer layer [38]. The energy gap of $Zn_{1-x}Cd_xS$ film can be tuned to minimize the conduction band alignment between a $Cu_2ZnSnS_4$ absorber and a buffer. As a result, the recombination decreased improving the open circuit voltage and fill factor efficiently.

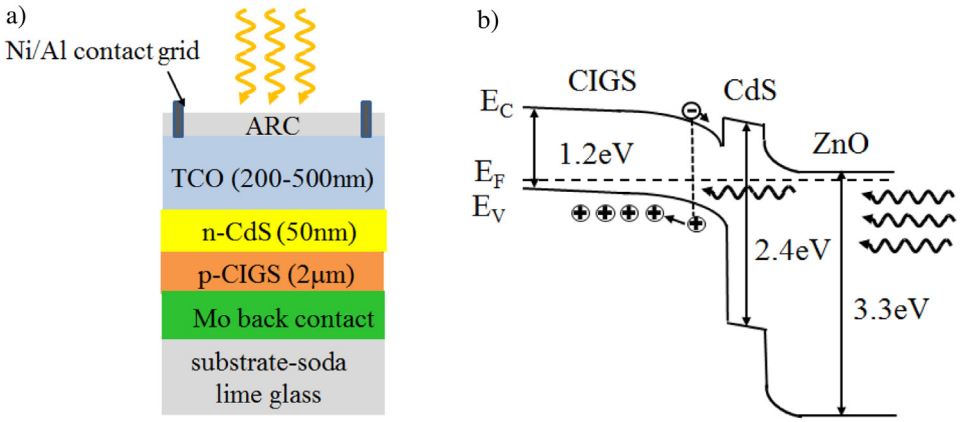


**Fig. 10.** (a) Layer structure and (b) band diagram of a conventional CIGS solar cell.

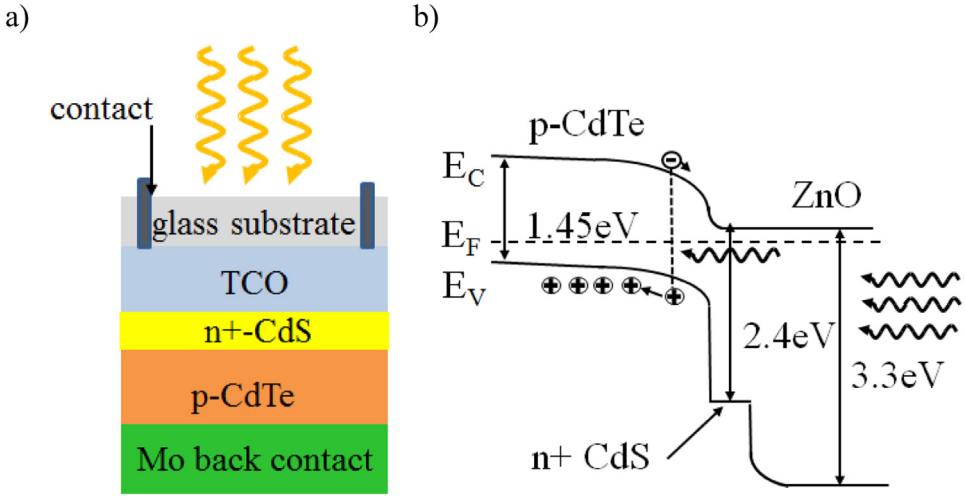


**Fig. 11.** (a) Layer structure and (b) band diagram of a CdTe solar cell.

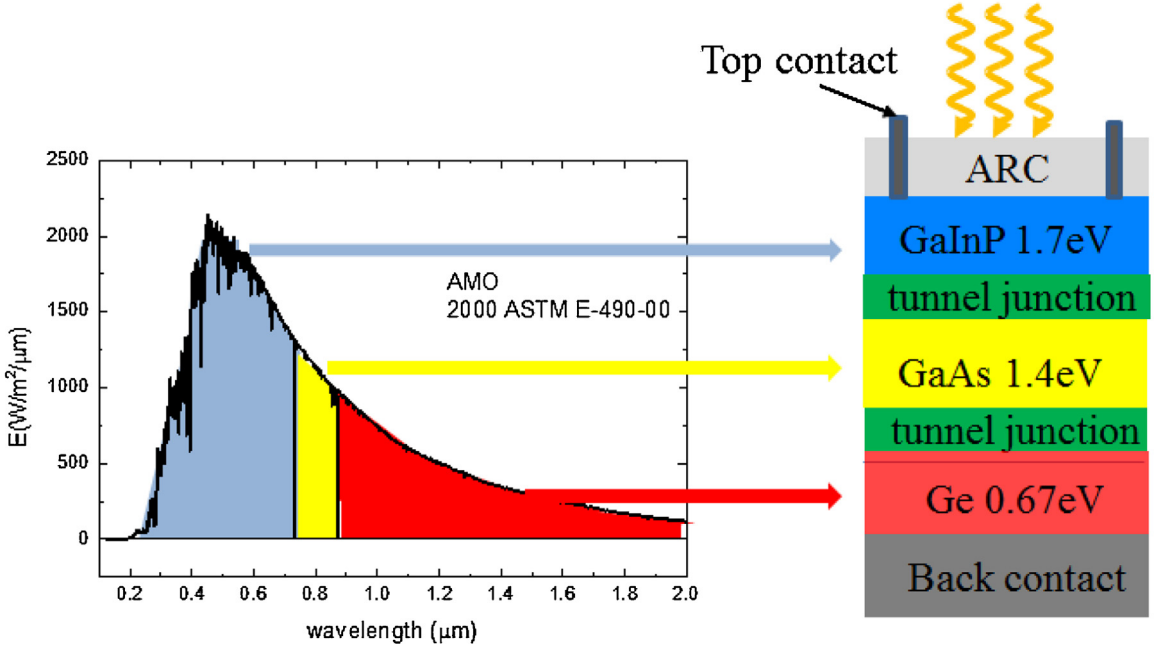


**Fig. 12.** Distribution of the AMO spectrum by the 3J solar cell and its layer structure.

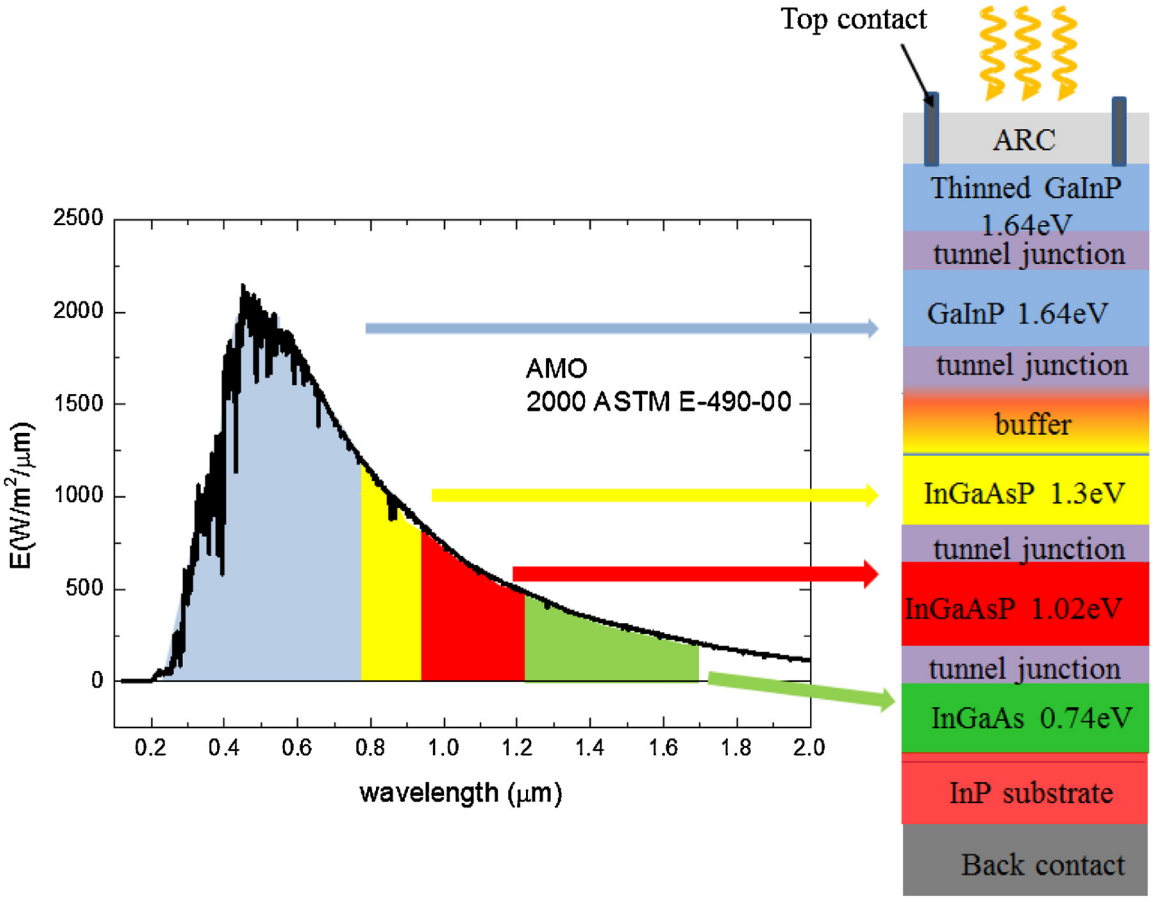


**Fig. 13.** Distribution of the AMO spectrum by the 5J solar cell and the layer structure of the cell.

*3.2.3. CdTe SC*

The record efficiency of 21% for a CdTe based SC belonged to First Solar since it was announced in 2014. In February 2016 First Solar announced new record – 22.1%. This result has been certified at the Newport Technology and Applications Center Lab, and recognized in NREL's most recent "Best Research Cell Efficiencies" reference chart [39]. CdTe is a II–VI direct band gap semiconductor of energy gap equal to 1.44 eV, very close to the optimal band gap energy [9]. The theoretical S–Q limit is equal to 33.5% (cf. Fig. 1). As grown CdTe is a p-type and in the HJ solar cells it serves as a p-type partner (absorber) to an n-type CdS. The structure and energy band diagram of typical CdTe/CdS HJ solar cells is presented in Fig. 11.

The record efficiency was obtained by doping the CdTe with phosphorus atoms [40] (the collaboration of National Renewable Energy Laboratory (NREL) with Washington State University and University of Tennessee researchers). The standard processing step using cadmium chloride has been replaced by inserting a small number of phosphorus atoms on tellurium lattice sites. This process has been followed by a careful formation of ideal interfaces between materials with different atomic spacing. Furthermore, the nanocrystalline CdS layers were deposited on CdTe. It was shown that in spite of the fact that they form non-ideal heterointerfaces with a 10% lattice mismatch they show excellent junction transport properties [40]. These results enable for the first time the fabrication of CdTe solar cells with an open-circuit voltage greater than 1 V.

*3.2.4. Multi-junction SC*

The concept of multijunction solar cells is based on the idea of converting the whole energy of a solar spectrum into electric energy. The simplest multijunction solar cell is composed of three (3J) junctions of three various energy gaps matching different parts of the solar spectrum (cf. Fig. 12). The highest energy band gap junction is located at the top of the 3J solar cell, the bottom cell is the cell with the lowest band gap and that of the middle energy gap is placed among them. Such a design is the result of the fact that the most energetic photons are absorbed close to the surface while the lower energy photons have larger penetration depths. Among these junctions, tunneling junctions are processed in order to prevent formation of reversely biased p–n junctions between top p-material and middle n-material, as well as between the middle p-material and bottom n material. The tunneling junctions are of wider band gap to prevent optical losses.

In Fig. 12 the partition of the AMO spectrum corresponding to the layer structure of the lattice matched $Ga_{0.5}In_{0.5}P/Ga_{0.99}In_{0.01}As/Ge$ 3J is shown.

The subcells are connected in series, therefore the total voltage equals the sum of voltages of the subcells whereas the current equals the minimum current out of the subcells. For such triple junction solar cells the efficiencies are approaching 40% under concentrated light [41]. The multijunction solar cells are very expensive and this limits their application to the space. In order to reduce their cost solar concentrators are used and, therefore, the efficiency for the MJ cells are usually measured under concentrated light. Concentrated sunlight usually increases the efficiency of a solar cell and reduces the solar-cell area, resulting in a lower cost due to a reduced amount of semiconductor material.

In order to reach higher efficiency, the number of subcells in MJ is increased. The best multijunction solar cells achieve the efficiency beyond the Shockley–Quiesser limit. The top five junction (5J) solar

cell record of efficiency 38.8% under a 1-sun illumination belongs to the Spectrolab and was announced in 2014 [42].

The cell voltage is comprised of 3.68 V from the top 3 junctions on GaAs of energy gap equal to 2.17, 1.68 and 1.4 eV and of 1.08 V from the bottom 2 junctions on InP of energy gap equal to 1.06 and 0.73 eV. These energy gaps are close to the optimal band gap combination for a 5J cell on InP, i.e. 2.1/1.64/1.3/1.02/0.74 eV (0.59, 0.76, 0.95, 1.21, 1.68 μm) [41]. The efficiency boost of this solar cell is due to the development of a specific wafer-bonding process for integrating InP- and GaAs-based materials. The bonding includes ternary and quaternary epilayers, enabling comfortably tuning of band gaps. Cell measurements at concentration indicate efficiencies approaching 41% at low concentration. Modeling indicates the potential to reach close to 47% at 500 suns [42].

In 2015 Suzhou Institute of Nano Tech and Nano Bionics announced 5J InGaP(1.64 eV)/InGaP(1.64 eV)/InGaAsP(1.3 eV)/InGaAsP(1.02 eV)/InGaAs(0.74 eV) solar cell structure on InP substrate [43]. Its efficiency as high as 46.2% is estimated under concentration at ~1500 suns. The layer structure of this solar cell is shown in Fig. 13. The bottom three subcells are lattice-matched to InP while the top two InGaP subcells are tensile-relaxed using metamorphic growth technology. Metamorphic growth means lattice-mismatched MJ. This technology demands buffer layers to fit in the lattice constants of neighboring p–n junctions.

### 3.2.5. *III–V/Si SC*

Recently scientists from the Energy Department's National Renewable Energy Laboratory (NREL) and from the Swiss Center for Electronics and Microtechnology (CSEM) announced a new world record for a tandem solar cell made of III–V/Si under a 1-sun solar irradiation [44]. They have elaborated a mechanically stacked GaInP/Si dual-junction solar cell. The solar cell is composed of a rear-heterojunction GaInP top cell and a HIT Si bottom cell. The two cells were made separately and then joined by mechanical stacking using glass as an electrically insulating optically transparent interlayer. The glass is a low-refractive-index material, which enhances the photon path length in the top cell. The cells operate independently (four terminal mode) and exhibit a total 1-sun efficiency of (29.8 ± 0.6)% (AM1.5 g). The scheme of the cell is shown in Fig. 14.

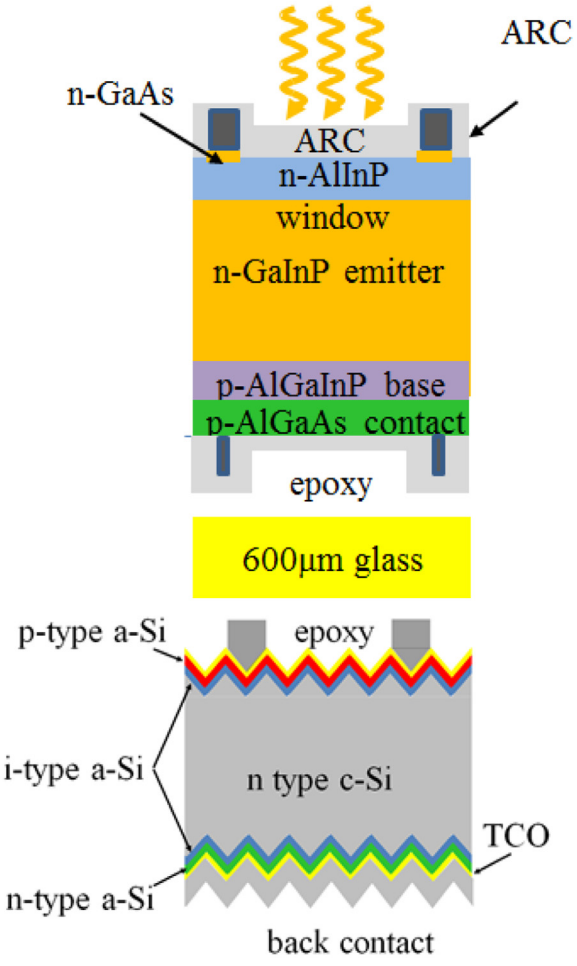


**Fig. 14.** The layer structure of the 5J solar cell.

## 4. New emerging technologies

In the past few decades several new technologies emerged which pave the way toward reducing the cost of a solar cell production. These are so called 3rd generation solar cells, but the technology is currently in its early stage so they do not play a role in the PV market entry, so far. These are organic, dye-sensitized (DSSC), perovskite and quantum dot cells. According to the solar cell efficiency tables [5] the record efficiency of the organic cells equals 11.2% and it belongs to Toshiba, 10.2015, and that of the DSSC – 11.9% and it was announced by Sharp, 09.2012. The status of these solar cells has been classified as an advanced demonstration, some products for sale [45]. There are numerous review articles concerning these cells, i.e. [32,46–49 and references therein]. As regards quantum dot and perovskite solar cells these technologies are in the commercial state called as "development and no products" [45]. For the quantum dot solar cells the record efficiency of 11.6% was announced recently by researchers from East China University of Science & Technology [50]. The review on perspectives of these solar cells can be found in [51–53] and references therein. Impressive rapid increase of perovskite solar cells efficiency starting from 3 to 4% in 2009 up to the recent record efficiency of 22.1% (the latter belongs to KRICT/UNIST, 03.2016) boosts this technology to the leading position out of all 3rd generation solar cells [54]. Perovskite solar cell technology was selected as one of the biggest scientific breakthroughs of 2013 by the editors of Science and Nature [55,56]. The review on the state of art and perspectives of perovskite solar cells' improvement is given in Refs. [54–59]. The number of references concerning the perovskite solar cells is huge – according to ISI Web of Knowledge this year it has already exceeded 1200 which testifies that this subject is at the center of interests of researchers all over the world and emphasis its significance. With perovskite solar cells there are still problems to be addressed. Among them the water solubility of perovskite based materials and the problem of scaling are listed as the main obstacles against their entry into the PV market.

Summing up, solar cell efficiency improvement has been one of the major concerns to produce the cost effective efficient solar cells. Among various solutions leading to the improvement of solar cell efficiency, plasmonic light trapping mechanism has been considered as promising solution for better photon harvesting. The review on the recent advances on the application of plasmonics in inorganic semiconductor solar cell efficiency improvements can be found, i.e., in Ref. [60] and references therein, while those concerning organic solar cells in Ref. [61]. An excellent review on perspectives of plasmon-enhanced solar energy is given in Ref. [62] and references therein. A brief overview of some of the key developments of the field of nanoplasmonics is given in [63].

## 5. Conclusions

In the paper the review on the top 1st and 2nd generation solar cells is elaborated. The presented examples of solar cells

were chosen from a vast number of solutions and many significant achievements are not addressed here. In the review the scheme of the layer structures are shown and for some of the cells, energy band diagrams are presented. The latter enables explanation of the efficiency improvements for relevant designs of solar cells. For a single junction solar cell there is still a lot of problems to be solved in order to approach the S–Q limit. Assuming that the problems with parasitic light absorption, recombination due to defects and resistive losses are overcome, the Auger recombination in Si solar cells poses an inevitable barrier for efficiency improvement. Considering thin films heterojunctions, CIGS and CdTe solar cells their efficiencies are also far from the S–Q limit in spite of the fact that these are direct band gap materials. The most promising is a tandem technology, i.e., the III–V/silicon tandem solar cell. Multijunction solar cells reach efficiency far above the S–Q limit but their technology is very expensive so that they are used only in space. Eventually the status of the 3rd generation of solar cells has been briefly reported. It has to be emphasized that nowadays the greatest hope of PV community is related with the latter generation, because it is bringing a breakthrough in a solar cells' technology, as the simplest and most cost effective out of all generations.

## Acknowledgements

This work has been partially supported by the Polish-Taiwanese/Taiwanese-Polish Joint Research Project DKO/PL-TW1/3/2013 and by the project of National Laboratory of Quantum Technologies (POIG. 02.02.00-00-003/08-00) and National Science Centre (DEC-2013/11/B/ST7/01385).

## References

[1] http://www.greentechmedia.com/articles/read/gtm-research-global-solar-pv-installations-grew-34-in-2015.
[2] http://resources.solarbusinesshub.com/solar-industry-reports/item/global-market-outlook-for-solar-power-2015-2019.
[3] http://www.pv-magazine.com/investors/module-price-index/.
[4] https://www.ise.fraunhofer.de/de/downloads/pdf-files/aktuelles/photovoltaics-report-in-englischer-sprache.pdf.
[5] M.A. Green, K. Emery, Y. Hishikava, W. Warta, E.D. Dunlop, Solar cell efficiency tables (version 48), Prog. Photovol.Res. Appl. 24 (2016) 905–913.
[6] http://www.itrpv.net/Reports/Downloads/2016/.
[7] M.A. Green, K. Emery, Y. Hishikawa, W. Warta, E.D. Dunlop, Solar cell efficiency tables (version 39), Prog. Photovol. Res. Appl. 20 (2012) 12–20.
[8] W. Shockley, H.J. Queisser, Detailed balance limit of efficiency of p–n junction solar cells, J. Appl. Phys. 32 (1961) 510–519.
[9] https://en.wikipedia.org/wiki/Shockley%E2%80%93Queisser_limit.
[10] J.H. Zhao, A.H. Wang, M.A. Green, 24.5% efficiency silicon PERT cells on MCZ substrates and 24.7% efficiency PERL cells on FZ substrates, Prog. Photovol. 7 (1999) 471–474.
[11] M.A. Green, The path to 25% silicon solar cell efficiency: history of silicon cell evolution, Prog. Photovol. 17 (2009) 183–189.
[12] K. Masuko, M. Shigematsu, T. Hashiguchi, D. Fujishima, M. Kai, N. Yoshimura, T. Yamaguchi, Y. Ichihashi, T. Mishima, N. Matsubara, T. Yamanishi, T. Takahama, M. Taguchi, E. Maruyama, S. Okamoto, Achievement of more than 25% conversion efficiency with crystalline silicon heterojunction solar cell, IEEE J. Photovol. 4 (2014) 1433–1435.
[13] D.D. Smith, P. Cousins, S. Westberg, R. De Jesus-Tabajonda, G. Aniero, Y.-C. Shen, Towards the practical limits of silicon solar cells, IEEE J. Photovol. 6 (2014) 1465–1469.
[14] R.M. Swanson, Approaching the 29% limit efficiency of silicon solar cells, in: Proc. 31st IEEE Photovoltaic Specialists Conference, Lake Buena Vista, FL, USA, 2005, pp. 889–894.
[15] A. Richter, M. Hermle, S.W. Glunz, Reassessment of the limiting efficiency for crystalline silicon solar cells, IEEE J. Photovol. 3 (2013) 1184–1191.
[16] S. Zhang, X. Pan, H. Jiao, W. Deng, J. Xu, Y. Chen, P.P. Altermatt, Z. Feng, P.J. Verlinden, 335 watt world record p-type mono-crystalline module with 20.6% efficient PERC solar cells, IEEE J. Photovol. 6 (2016) 145–152.
[17] R. Swanson, The role of modeling in SunPower's commercialization efforts, in: Presented at Challenges in PVscience, Technology, and Manufacturing: A workshop on the Role of Theory, Modeling and Simulation, Purdue University, August 2–3, 2012.
[18] D. Macdonald, L.J. Geerligs, Recombination activity of interstitial iron and other transition metal point defects in p- and n-type crystalline silicon, Appl. Phys. Lett. 85 (2004) 4061–4063.
[19] http://www.trinasolar.com/ap/about-us/newinfo_1076.html.
[20] Thin Film Solar Cells: Fabrication, Characterization and Applications, in: J. Poortmans, V. Arkhipov (Eds.), John Wiley & Sons, Inc, Hoboken, NJ, USA, 2006.
[21] T.F. Schulze, L. Korte, F. Ruske, B. Rech:, Band lineup in amorphous/crystalline silicon heterojunctions and the impact of hydrogen microstructure and topological disorder, Phys. Rev. B 83 (2011), 165314-1–165314-11.
[22] S. Xiao, S. Xu, High-efficiency silicon solar, cells—materials and devices physics, Crit. Rev. Solid State Mater. Sci. 39 (2014) 277–317.
[23] O.D. Miller, E. Yablonovitch, S.R. Kurtz, Intense internal and external fluorescence as solar cells approach the Shockley–Queisser efficiency limit, IEEE J. Photovol. 2 (2012) 303–311.
[24] B.M. Kayes, H. Nie, R. Twist, S.G. Spruytte, F. Reinhardt, I.C. Kizilyalli, G.S. Higashi, 27.6% conversion efficiency, a new record for single-junction solar cells under 1 sun illumination, in: Proceedings of the 37th IEEE Photovoltaic Specialists Conference, IEEE, 2011, pp. 000004–000008.
[25] T. Matsui, H. Sai, T. Suezaki, M. Matsumoto, K. Saito, I. Yoshida, M. Kondo, Development of highly stable and efficient amorphous silicon based solar cells, Proc. 28th European Photovoltaic Solar Energy Conference (2013) 2213–2217.
[26] R.A. Street, Hydrogenated Amorphous Silicon, Cambridge University Press, UK, 1991.
[27] PV Magazine, 15th June 2016.
[28] http://www.hanergyapac.com/en/media-center/press-release/100-news-006.
[29] M. Contreras, L. Mansfield, B. Egaas, J. Li, M. Romero, R. Noufi, E. Rudiger-Voigt, W. Mannstadt, 37th IEEE Photovoltaic Specialists Conference (PVSC), 2011, pp. 000026–000031.
[30] R. Scheer, H.W. Schock, Chalcogenide Photovoltaics, Wiley-VCh Verlag, Weinheim, Germany, 2011 (Chapter 2).
[31] M. Ruckh, D. Schmid, H.W. Schock, Photoemission study of the ZnO/CdS interface, J. Appl. Phys. 76 (1994) 5945–5948.
[32] M.D. Archer, M.A. Green, Clean Electricity from Photovoltaics, Imperial College Press, 2015.
[33] A. Klein, Energy band alignment in chalcogenide thin film solar cells from photoelectron spectroscopy, J. Phys.: Condens. Matter 27 (2015) 134201–134225.
[34] J. Hedström, H. Ohlsen, M. Bodegard, A. Kylner, L. Stolt, D. Hariskos, M. Ruckh, H.W. Schock, ZnO/CdS/Cu(In,Ga)$Se_2$ thin film solar cells with improved performance, Proceedings of 23rd IEEE Photovoltaic Specialists Conference (1993) 364–371.
[35] F. Pianezzi, P. Reinhard, A. Chirilă, B. Bissig, S. Nishiwaki, S. Buecheler, A.N. Tiwari, Unveiling the effects of post-deposition treatment with different alkaline elements on the electronic properties of CIGS thin film solar cells, Phys. Chem. Chem. Phys. 16 (2014) 8843–8851.
[36] A. Chirilă, P. Reinhard, F. Pianezzi, P. Bloesch, A.R. Uhl, C. Fella, L. Kranz, D. Keller, C. Gretener, H. Hagendorfer, D. Jaeger, R. Erni, S. Nishiwaki, S. Buecheler, A.N. Tiwari, Potassium-induced surface modification of Cu(In,Ga)$Se_2$ thin films for high-efficiency solar cells, Nat. Mater. 12 (2013) 1107–1111.
[37] G. Larramona, S. Levcenko, S. Bourdais, A. Jacob, C. Choné, B. Delatouche, C. Moisan, T. Unold, G. Dennler, Fine-tuning the Sn content in CZTSSe thin films to achieve 10.8% solar cell efficiency from spray deposited water–ethanol-based colloidal inks, Adv. Energy Mater. 4 (2015) 1501404–1501414.
[38] K. Sun, C. Yan, F. Liu, J. Huang, F. Zhou, J.A. Stride, M. Green, X. Hao, Over 9% efficient kesterite $Cu_2ZnSnS_4$ solar cell fabricated by using $Zn_{1-x}Cd_xS$ buffer layer, Adv. Energy Mater. 6 (2016) 1600046–1600052.
[39] http://www.greentechmedia.com/articles/read/First-Solar-Hits-Record-22.1-Conversion-Efficiency-For-CdTe-Solar-Cell.
[40] J.M. Burst, J.N. Duenow, D.S. Albin, E. Colegrove, M.O. Reese, J.A. Aguiar, C.-S. Jiang, M.M. Al-Jassim, D. Kuciauskas, W.K. Metzger, M.K. Patel, S. Swain, T. Ablekim, K.G. Lynn, CdTe solar cells with open-circuit voltage breaking the 1 V barrier, Nature Energy 1 (2016), 16015.
[41] J.H. Ermer, R.K. Jones, P. Hebert, P. Pien, R.R. King, D. Bhusari, R. Brandt, O. Al-Taher, C. Fetzer, G.S. Kinsey, N. Karam, Status of C3MJ+ and C4MJ production concentrator solar cells at spectrolab, IEEE J. Photovol. 2 (2012) 209–213.
[42] P.T. Chiu, D.C. Law, R.L. Woo, S.B. Singer, D. Bhusari, W.D. Hong, A. Zakaria, J. Boisvert, S. Mesropian, R.R. King, N.H. Karam, 35.8% space and 38.8% terrestrial 5 J direct bonded cells, in: Proc. 40th IEEE Photovoltaic Specialist Conference, Denver, 2014, pp. 11–13.
[43] Y. Huang, H. Yang, Design of InP-based metamorphic high efficiency five-junction solar cells for concentrated photovoltaics, Semicond. Sci. Technol. 30 (2015) 105031–105038.
[44] S. Essig, M.A. Steiner, C. Allebe, J.F. Geisz, B. Paviet-Salomon, S. Ward, A. Descoeudres, V. LaSalvia, L. Barraud, N. Badel, A. Faes, J. Levrat, M. Despeisse, C. Ballif, P. Stradins, D.L. Young, Realization of GaInP/Si dual-junction solar cells with 29.8% 1-sun efficiency, IEEE J. Photovol. 6 (2016) 1012–1019.
[45] M. Jacoby, The future of low-cost solar cells, Chem. Eng. News 94 (2016) 30–35.
[46] H. Lu, X. Xu, Z. Bo, Perspective of a new trend in organic photovoltaic:ternary blend polymer solar cells, Sci. China Mater. 59 (2016) 444–458.
[47] M.-E. Ragoussia, T. Torres, New generation solar cells: concepts, trends and perspectives, Chem. Commun. 51 (2015) 3957–3972.
[48] W.-Y. Rho, H. Jeon, H.-S. Kim, W.-J. Chung, J.S. Suh, B.-H. Jun, Recent progress in dye-sensitized solar cells for improving efficiency: $TiO_2$ nanotube arrays in active layer 2, J. Nanomater. 2015 (2015) 1–17.

[49] A. Hagfeldt, G. Boschloo, L. Sun, L. Kloo, H. Pettersson, Dye-sensitized solar cells, Chem. Rev. 110 (2010) 6595–6663.
[50] J. Du, Z. Du, J.-S. Hu, Z. Pan, Q. Shen, J. Sun, D. Long, H. Dong, L. Sun, X. Zhong, L.-J. Wan, Zn–Cu–In–Se quantum dot solar cells with a certified power conversion efficiency of 11.6%, J. Am. Chem. Soc. 138 (2016) 4201–4209.
[51] Z. Zheng, H. Ji, P. Yu, Z. Wang, Recent progress towards quantum dot solar cells with enhanced optical absorption, Nanoscale Res. Lett. 11 (2016) 266–273.
[52] J. Wu, S. Chen, A. Seeds, H. Liu, Quantum dot optoelectronic devices: lasers, photodetectors and solar cells, J. Phys. D 48 (2015) 363001–363026.
[53] I. Ramiro, A. Marti, E. Antolin, A. Luque, Review of experimental results related to the operation of intermediate band solar cells, IEEE J. Photovol. 4 (2014) 736–748.
[54] J. Seo, J.H. Noh, S.I. Seok, Rational strategies for efficient perovskite solar cells, Acc. Chem. Res. 49 (2016) 562–572.
[55] Science News, Newcomer juices up the race to harness sunlight, Science 342 (2013) 1438–1439.
[56] Nature News Features, Henry Snaith: Sun worshipper, Nature 504 (2013) 357–365.
[57] W.S. Yang, J.H. Noh, N.J. Jeon, Y.C. Kim, S. Ryu, J. Seo, S.I. Seok, High-performance photovoltaic perovskite layers fabricated through intramolecular exchange, Science 348 (2015) 1234–1237.
[58] N.-G. Park, Perovskite solar cells: an emerging photovoltaic technology, Mater. Today 18 (2015) 66–72.
[59] P.P. Boix, K. Nonomura, N. Mathews, S.G. Mhaisalkar, Current progress and future perspectives for organic/inorganic perovskite solar cells, Mater. Today 17 (2014) 16–23.
[60] P. Mandal n, S. Sharma, Progress in plasmonic solar cell efficiency improvement: a status review, Renew. Sustain. Energy Rev. 65 (2016) 537–552.
[61] W.R. Erwin, H.F. Zarick, E.M. Talbert, R. Bardhan, Light trapping in mesoporous solar cells with plasmonic nanostructures, Energy Environ. Sci. 9 (2016) 1577–1601.
[62] S.K. Cushing, N. Wu, Progress and perspectives of plasmon-enhanced solar energy conversion, J. Phys. Chem. Lett. 7 (2016) 666–675.
[63] M.L. Brongersma, Introductory lecture: nanoplasmonics, Faraday Discuss 178 (2015) 9–36.